


Highly excited neutral molecules and fragment atoms of H₂ induced by strong laser fields

Tian Sun,¹ Lei Zhao,² Yang Liu,¹ Jing Guo¹,, Hang Lv,^{1,*} and Haifeng Xu^{1,†}

¹*Institute of Atomic and Molecular Physics, Jilin University, Changchun 130012, China*

²*School of Science, Northeast Electric Power University, Jilin 131200, China*

 (Received 7 November 2022; revised 17 April 2023; accepted 19 July 2023; published 31 July 2023)

We experimentally investigate the Rydberg state excitation (RSE) process of H₂ molecules induced by a strong laser field in the tunneling ionization region. Both neutral parent molecules H₂ and fragment atoms H are observed to survive the strong 800-nm femtosecond laser fields in high Rydberg states; however, their behaviors are quite different upon varying the laser intensity and laser ellipticity. The results are compared to single and double ionization as well as RSE from the companion atom Ar. Analysis indicates that the H₂ RSE is produced by the recapture or frustrated tunneling ionization process, and the nonsequential double ionization of H₂ induced by recollision of the tunneled electrons plays an important role in the fragment H RSE of H₂ in strong laser fields.

DOI: [10.1103/PhysRevA.108.013120](https://doi.org/10.1103/PhysRevA.108.013120)

I. INTRODUCTION

In a strong laser field with intensity larger than 10^{13} W/cm², an outmost electron in an atom or a molecule can be liberated via tunneling the barrier formed by a combination of the Coulomb potential and the laser electric field. Tunneling ionization generally acts as the initial step of various strong-field physical processes of atoms and molecules. According to the well-known three-step recollision scenario [1,2], the tunneled electron is accelerated and may be driven back to recollide to the core in an oscillating laser field, inducing various highly nonlinear phenomena such as high-order-harmonic generation [3,4], high-order above-threshold ionization [5,6], and nonsequential double ionization (NSDI) [7]. Alternatively, it is interesting to find both theoretically [8] and experimentally [9] that the tunneled electron may also be recaptured by the ionic Coulomb potential into a Rydberg state, producing a highly excited neutral atom. Such a Rydberg state excitation (RSE) process in strong laser fields, also known as frustrated tunneling ionization (FTI) [9], provides an important complementary aspect of the picture of strong-laser-atom/molecule interaction, and it can potentially be applied in neutral particle acceleration [10,11] and as an ultrafast coherent light source [12–15], thus it has been the subject of elaborate experimental and theoretical studies during the past decade [16–23].

Most studies are performed on the strong-field RSE of atoms, in which capture probability has been investigated in detail in different laser fields, and the underlying physics of the recapture has been investigated. It is now indicated that the atomic RSE is a coherent recapture process accompanying above-threshold ionization, according to the fully

quantum-mechanical model proposed recently by Hu *et al.* [22]. In addition to FTI, the frustrated double ionization (FDI) of atoms has also been identified. A double-hump photoelectron momentum distribution generated from Ar FDI has been observed in a recent experiment [24], and it is confirmed to be due to recollision by a three-dimensional (3D) semiclassical perspective [25]. It has been demonstrated that the atomic FDI is a general strong-field physical process that could be accompanied with NSDI in the context of a recollision scenario.

On the other hand, our knowledge about the molecular RSE induced by a strong laser field is rather limited. By investigating the corresponding kinetic energy releases of different fragment channels, several studies have identified a highly excited neutral atom produced from dissociative ionization or Coulomb explosion in strong laser fields for diatomic molecules (e.g., H₂/D₂ [26–29], N₂ [30], CO [31], O₂ [32]) as well as dimers (e.g., Ar₂ [33], N₂Ar [34,35]). It is indicated that the RSE of the neutral atom is produced via the neutralization of fragment ions by recapturing the tunneled electrons into the highly excited states. Such a phenomenon, dubbed frustrated dissociative double ionization, has been indicated as a sequential process (e.g., $D_2 + n\hbar\omega \rightarrow D_2^+ + e_1 + m\hbar\omega \rightarrow D^+ + D^+ + e_2 \rightarrow D^+ + D^* + e$) as most of the studies are carried out in high laser intensity over 10^{15} W/cm² where sequential double ionization generally dominates [28,29]. Whether the NSDI or the recollision plays a role in the formation of the atomic fragment RSE remains unknown. Moreover, while various studies have shown that the structure of a molecular orbital plays a pivotal role in tunneling ionization as well as the recollision-induced physical processes in strong laser fields [36–40], such an effect in molecular RSE still needs to be addressed. Recent studies have shown that neutral diatomic molecules (N₂ and O₂) can also survive strong 800-nm laser fields in high Rydberg states, and their behaviors are remarkably different compared to atoms, which can be well understood in the frame of the

*lvhang811@jlu.edu.cn

†xuhf@jlu.edu.cn

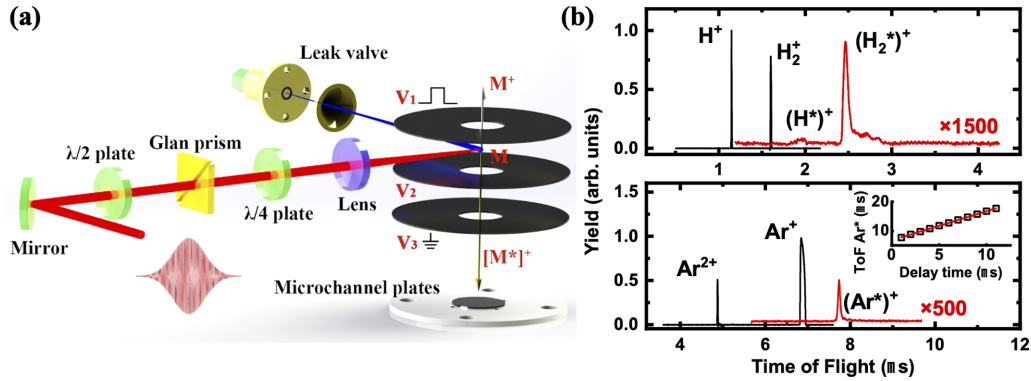


FIG. 1. (a) Schematic diagram of the experimental setup for investigation of the RSE process. (b) Typical MS spectra for direction ionization and RSE processes of H_2 and Ar irradiated by a linearly polarized 800 nm strong laser field with a laser intensity of $290 \text{ TW}/\text{cm}^2$. The inset shows the dependence of $(Ar^*)^+$ time-of-flight on the ΔT value. See text for details.

recapture picture together with their different structures of molecular orbitals [18,41].

In this paper, we experimentally investigate the strong-field RSE process of H_2 molecules in the tunneling ionization region, using a pulsed-field-ionization method combined with a time-of-flight mass spectrometer (PFI-TOF MS). Both highly excited neutral parent molecules (H_2^*) and fragment atoms (H^*) are observed after H_2 molecules are irradiated by strong 800-nm laser fields, which present a remarkably different dependence on laser intensity and ellipticity. We compare RSE to single and double strong field ionization as well as RSE of the companion atom Ar [the atom with the ionization potential (I_p) value that is similar to that of the molecule H_2]. It is indicated that the molecular RSE is produced by the recapture process, and recollision of the tunneling electrons plays a role in the fragment RSE process in strong laser fields.

II. EXPERIMENTAL SETUP

In Fig. 1(a), we show schematically the experimental setup for investigation of the RSE process, which is accomplished by PFI-TOF MS. Briefly, an atomic or molecular beam is introduced into the reaction chamber through a $10 \mu\text{m}$ leak valve and a skimmer with a stagnation pressure at 1 atm. The background pressure without gas injection is less than $1 \times 10^{-6} \text{ Pa}$ and the working pressure is around $1 \times 10^{-4} \text{ Pa}$ in the reaction chamber. The laser system used in the study is a Ti:sapphire femtosecond laser with a central wavelength of 800 nm, a pulse duration of 50 fs, a repetition rate of 1 kHz, and a maximum pulse energy of 4 mJ. A half-wave plate and a Glan prism are employed to continuously adjust the laser intensity. A quarter-wave plate is used to change the polarization of the laser. In the ellipticity-dependent experiments, we fix the major axis of the laser polarization and change the ellipticity by rotating the half-wave plate placed before the quarter-wave plate. The laser beam is focused into the vacuum chamber with a 250 mm focusing lens to interact with the atomic/molecular beam. The laser intensity is calibrated by comparing the measured saturation intensity of Ar with that calculated by the Ammosov-Delome-Krainov (ADK) model [42].

In our PFI experiments, any direct ionized ions (M^{m+} , $M = H_2, \text{Ar}, \text{or } H, m = 1 \text{ or } 2$) after atoms or molecules

irradiated by the strong field are pushed away from the detector by a dc electric field. After a delay time ΔT , the remaining highly excited neutrals (M^*) are then field-ionized by switching the voltage of the repeller plate V_1 , and the resulting ions (M^*) $^+$ are detected by dual microchannel plates at the end of the flight of about 50 cm. In this way, the neutral Rydberg states with principal numbers $20 < n < 30$ are detected, estimated by a saddle-point model of static field ionization [$F = 1/(9n^4)$, F is the electric field]. In the case for detection of direct ionization, M^{m+} , standard dc electric fields are applied in the TOF-MS, with the voltages kept the same as those in detecting $(M^*)^+$ to ensure identical detection efficiencies. Typical MS spectra are presented in Fig. 1(b) for M^{m+} and $(M^*)^+$ with a $\Delta T = 1 \mu\text{s}$. The inset shows the dependence of $(Ar^*)^+$ time-of-flight on the ΔT value, which exhibits an excellent linear relationship indicating the signal is generated by PFI of the highly excited neutral Rydbergs. While the yield of $(Ar^*)^+$ or $(H_2^*)^+$ changes slightly upon increasing ΔT , that of $(H^*)^+$ decreases dramatically at $\Delta T \geq 1 \mu\text{s}$ using the PFI-TOF MS technique, thus in the intensity- and ellipticity-dependent measurements presented in the following sections, ΔT is kept at $0.5 \mu\text{s}$ for a good signal-to-noise ratio.

III. RESULTS AND DISCUSSION

A. Formation of the highly excited neutral molecules

In our PFI-TOF MS experiments, we observe that both H atoms and H_2 molecules survived in highly excited Rydberg states (H^* and H_2^*) after being irradiated by linearly polarized 800-nm strong femtosecond laser fields [see Fig. 1(b)]. The probability of the RSE process depends strongly on laser intensity and ellipticity. In Fig. 2(a), we show the measured ion yields from PFI of Rydbergs H^* and H_2^* as a function of laser intensity in the range of 90–600 TW/cm^2 . For comparison, the results of the companion atom Ar are also presented in the figure. In the laser intensities investigated in the present study, the Keldysh adiabatic parameter γ is typically less than 1 ($\gamma = \sqrt{I_p/2U_p}$, where $U_p = E^2/4\omega^2$ is the ponderomotive energy, and E and ω are the electric intensity and frequency of the laser field, respectively), indicating that the ionization is dominated by the tunneling ionization.

As shown in Fig. 2(a), the $(H_2^*)^+$ yield is apparently lower than that of $(Ar^*)^+$ in the laser intensity range investigated in

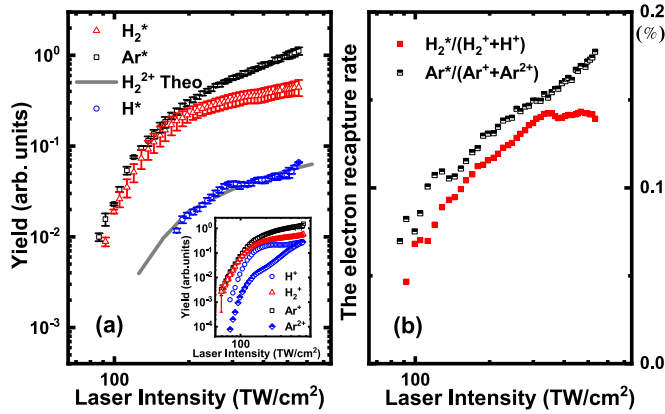


FIG. 2. (a) Dependence of the RSE yields on the laser intensity for H₂ and Ar after being irradiated by linearly polarized laser fields. The solid line shows the calculated double ionization yields of H₂ molecules. The inset shows the results of direct ionization for H₂ and Ar. Error bars are standard deviation from three independent measurements. (b) The electron recapture rate $[(M^*)^+/M^{n+}]$ as a function of laser intensity. See text for details.

the study. This finding, i.e., the suppressed RSE in H₂ compared to its companion atom Ar, is similar to that in the case of strong field ionization, as shown in the inset of Fig. 2(a), which quantitatively reproduces the result reported in the literature [43,44] and indicates the suppression in ionization of the H₂ molecule compared to Ar. The ratios of $(M^*)^+$ to ionization M^{n+} for both the molecule and the atom are presented in Fig. 2(b), which qualitatively represents the electron recapture rate as a function of laser intensity. Note that while the measured ratio is around 0.05–0.15 %, the total recapture rate should be much higher, since only those Rydbergs with $20 < n < 30$ are detected in the present study, and they correspond to less than 2% of the total recapture rate estimated by the semiclassical calculations by Nubbemeyer [9]. One can see that the ratio for the H₂ molecule is apparently lower than that for the Ar atom, indicating the suppressed recapture rate of the molecule. According to previous theoretical studies [45–49], the origin of the suppressed ionization of H₂ could be attributed to an interplay of three reasons, i.e., the spatial geometrical configurations of the outermost molecular orbital, the intramolecular interference effect, and the difference in the vertical and ground state I_p due to the large difference in equilibrium internuclear distance for H₂⁺ and H₂. The fact that the appearance of the suppression in the RSE is accompanied by ionization indicates that the molecular RSE is related to strong field ionization, that is, the highly excited neutral molecule induced by strong laser fields comes from the photoelectron that first tunnels out and then is recaptured in Rydberg states by the Coulomb potential. Our results indicate that the molecular structure plays a similarly important role in the RSE process as in the strong field ionization.

We further investigate the molecular RSE in elliptically polarized laser fields. As shown in Fig. 3(a), the probability of H₂ RSE depends strongly on the laser ellipticity ε and is completely suppressed when ε is larger than 0.5. Our results show that the RSE of H₂ molecules exhibits a similar laser ellipticity dependence to that of its companion atom

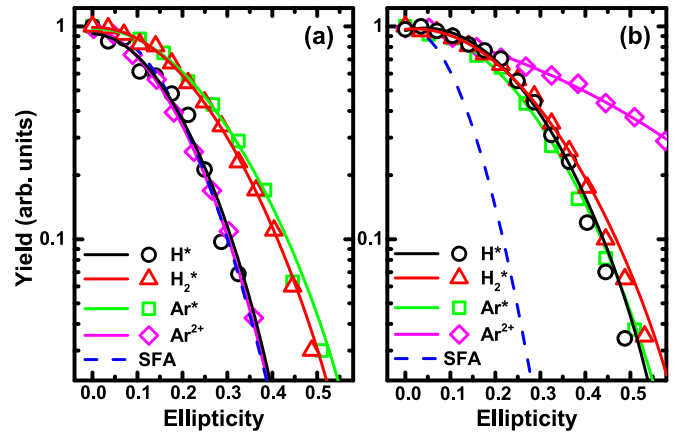


FIG. 3. Dependence of the yields of H* (black circle), H₂* (red triangle), Ar* (green square), and Ar²⁺ (pink diamond) on the laser ellipticity. (a) 200 TW/cm², (b) 500 TW/cm². Solid lines are the Gaussian fitting of the experimental results. The blue dashed line is the analytical results based on the SFA model (see text).

Ar, which has a well-defined Gaussian-type profile with a full width at half-maximum (FWHM) of 0.45. [For Ar, the FWHM is 0.48. See the solid lines in Fig. 3(a) for the Gaussian fitting results.] On the other hand, the H₂ RSE yields present a much weaker dependence on the laser ellipticity compared to the analytical result derived by Landsman *et al.* [19] based on the strong field approximation (SFA) model [see the blue dashed line in Fig. 3(a)]. The SFA model for RSE is analogous to the tunneling-plus-recollision phenomena, giving the distribution $P_R(\varepsilon)$ upon changing the laser ellipticity ε as $P_R(\varepsilon) \approx P_R(\varepsilon = 0) \exp(-\frac{1.25\sqrt{2I_p E}}{\omega^2} \varepsilon^2)$, which well reproduces the Ar NSDI results [see the Ar²⁺ results in Fig. 3(a)]. The apparent difference between the ellipticity dependence of H₂* and that of the SFA model indicates that the molecular RSE is not a tunneling-plus-recollision process as NSDI. Indeed, the weaker ellipticity dependence of RSE compared to recollision-induced processes like NSDI has also been observed in atoms (Ar and Kr), as investigated in detail by Zhao *et al.* in their joint experimental and theoretical study [50]. Their analysis indicates that the Coulomb effect plays an important role in the strong-field atomic RSE process, and more importantly, instead of understanding it in the framework of the tunneling-plus-recollision scenario, the strong dependence of the RSE probability on the laser ellipticity is explained by the fact that the yields of electrons with low kinetic energy that can be captured in Rydberg states decrease in elliptically polarized laser fields [50]. The similar ellipticity dependence of H₂* versus Ar* observed in the present study further implies that the molecular RSE is also produced by recapture of the tunneled electrons with low kinetic energy into highly excited Rydberg states.

B. Formation of the highly excited fragment atoms

We now turn to discuss the RSE of an H fragment atom induced by strong laser fields. The experimentally measured (H*)⁺ yields are also presented in Figs. 2 and 3 upon varying laser intensity and ellipticity, respectively. It can be seen that

the strong-field RSE of the fragment hydrogen atoms behaves quite differently compared to that of the parent H_2 molecules. As shown in Fig. 2(a), the intensity dependence of the $(H^*)^+$ yields presents a kneelike structure (i.e., a weak dependence on the laser intensity) at around 200 TW/cm^2 . Such a knee structure in the intensity-dependence curve is a signature of NSDI induced by linearly polarized strong laser fields. Note such a structure in the intensity-dependence curve of Ar^{2+} shown in the inset of Fig. 2. To further reveal the relation between the H^* formation and the NSDI process, we perform a theoretical calculation using the 3D classical ensemble method instead of experimental measurement, since doubly charged ions H_2^{2+} are unstable and cannot be detected by a mass spectrometer. A detailed description of the theoretical method of the strong-field double ionization of H_2 is presented in the Appendix. The calculated H_2^{2+} yield as a function of laser intensity is plotted in Fig. 2(a) as a solid line. It can be seen that the intensity dependence of the $(H^*)^+$ yield resembles the calculated H_2^{2+} result, indicating that the RSE of the fragment H atom could be related to the dissociation of H_2^{2+} in strong laser fields.

The probability of the fragment H RSE exhibits a much stronger dependence on the laser ellipticity compared to that of the molecular RSE at a laser intensity around 200 TW/cm^2 , as shown in Fig. 3(a). Interestingly, the ellipticity dependence of H^* is consistent with the analytical result based on SFA as well as that of the measured Ar^{2+} results at $\sim 200 \text{ TW/cm}^2$. Note that at this laser intensity, NSDI would be the dominant process in the strong field double ionization of Ar. Such a strong dependence on the laser ellipticity is in accordance with the tunneling-plus-recollision (or three-step recollision) scenario, in which the probability for the recollision diminishes with increasing laser ellipticity due to the greater drift momentum spread of the returning electron wave packet. On the other hand, as we have mentioned above, the FTI process is unlike the tunneling-plus-recollision phenomena since the tunneled electron does not need to return to the tunneling exit to be captured into Rydbergs, thus it presents a weaker dependence on the laser ellipticity [see the results of H_2^* and Ar^* in Fig. 3(a)] compared to recollision-induced phenomena such as NSDI. The fact that the ellipticity dependence of H^* resembles the SFA prediction and the Ar NSDI result strongly indicates that the H RSE is produced via a frustrated dissociative NSDI of H_2 , that is, after NSDI in strong laser fields, the unstable doubly charged ion H_2^{2+} immediately dissociates, and one of the product H^+ captures an electron in the way it goes out to form H^* . Thus, as in NSDI, the H^* yields show a much stronger dependence on the laser ellipticity, which is well reproduced by the prediction of the SFA model as shown in Fig. 3(a).

It should be mentioned that at high laser intensities ($\geq 500 \text{ TW/cm}^2$), a sequential DI (SDI) process in which two electrons are released one by one would be dominant in double ionization of atoms Ar and molecules H_2 . As shown in Fig. 3(b), for the results measured at a laser intensity of 500 TW/cm^2 , the yield of Ar^{2+} from SDI exhibits a weak dependence on the laser ellipticity, and that of H^* deviates from the SFA prediction, which is unlike that in Fig. 3(a) and is consistent with the results of H_2^* and Ar^* , indicating that H RSE resembles the FTI mechanism without any relation

to the recollision, as already discussed in both experimental measurements [28–30] and theoretical investigations [27].

It is well known that there are two pathways for NSDI in strong laser fields. In the recollision impact ionization (RII) pathway, the second electron in an atom or molecule is directly ionized upon collision with the returning first electron, while in the recollision-induced excitation with subsequent field ionization (RESI) pathway, the recolliding electron returns to the core and transfers energy to the second electron to excite to an excited state, which is subsequently tunneling-ionized at a delay of more than 0.4 optical cycle. To examine which pathway contributes to the frustrated dissociative NSDI of H_2 , we analyze the trajectories of all NSDI events in our 3D classical calculations. We present in Fig. 4(a) the calculated momentum distributions of the correlated electrons from double ionization of the H_2 molecules. The results indicate that both RII and RESI pathways contribute to the NSDI of H_2 . The momenta distributed in the first and third quadrants with a clear fingerlike structure are due to the RII process [51,52], while those in the second and fourth quadrants could be attributed to the RESI process. Two typical types of energy evolution of electrons in NSDI as a function of time are presented in Figs. 4(b) and 4(c). Here the direction of the linearly polarized laser field is arranged along the molecular axis. E_1 , E_2 , and E_p represent the energy of the first electron, the second electron, and the Coulomb repulsive energy between two electrons, respectively. A sharp peak in E_p appears at the time of recollision, which is due to the electron-electron correlation in the NSDI process. We can see from Fig. 4(b) that electron 1 is ionized immediately after recollision, and electron 2 is first excited and then ionized after about half of an optical cycle, which represents the RESI process. In Fig. 4(c), both electrons 1 and 2 are ionized immediately after recollision, representing the RII process. It is noted that those electrons with low final kinetic energy E_k (typically $0 < E_k < 0.4 \text{ eV}$) are preferred to be captured in Rydbergs [50]. We find that among all the NSDI events with a final E_k of an electron less than 0.4 eV, over 87% of the trajectories present a similar energy evolution to that shown in Fig. 4(b). This finding indicates that the frustrated dissociative NSDI of H_2 is related to the RESI pathway.

The above results strongly indicate that the recollision plays an essential role in the H RSE process in the NSDI region, that is, the H RSE observed in the present study is produced via the frustrated dissociative NSDI of H_2 . It is worth mentioning that for H_2 , dissociative ionization via bond softening (BS) and charge-resonant enhanced ionization (CREI) could be a dominant process over NSDI to produce H^+ at a laser intensity below 300 TW/cm^2 . This could be the reason that the H^+ signals show no knee structure (a signature of NSDI) in the intensity-dependent measurements [see the inset of Fig. 2(a)]. On the other hand, the relatively minor recollision-induced channels can be distinguished in multi-cycle strong laser fields by selecting molecular alignment perpendicular to the laser polarization, a case in which both BS and CREI channels would be greatly suppressed, as discussed in previous studies on strong field ionization [53–55]. In our study on the RSE process, considering that the atom fragments carry kinetic energy typically higher than 0.5 eV, only those aligned close to the perpendicular direction can be

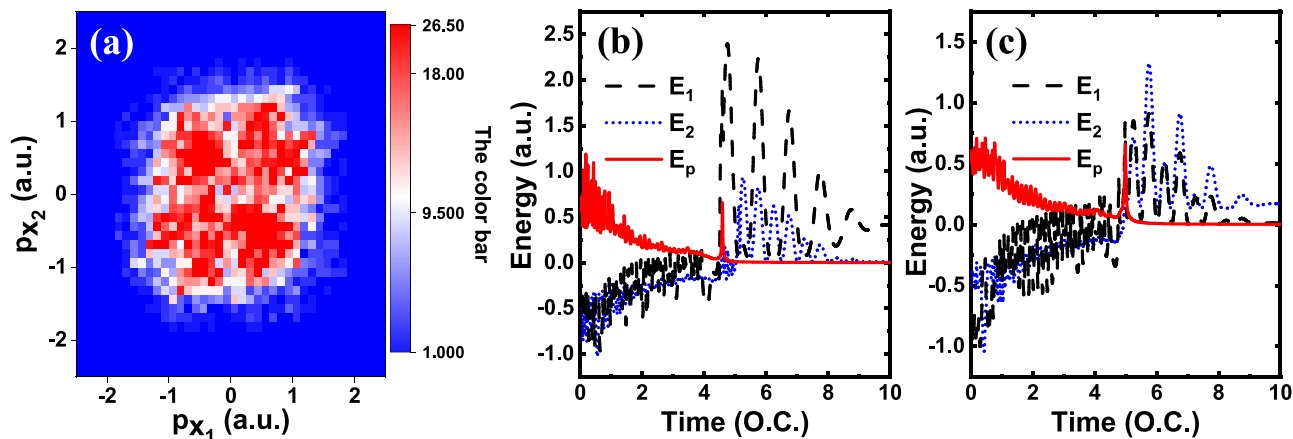


FIG. 4. (a) Calculated momentum distributions of the correlated electrons from double ionization of the H_2 molecules. (b), (c) Two typical types of energy evolution of electrons in NSDI as a function of time.

detected by the delayed-field ionization TOF-MS method (a typical delay time ΔT of $0.5 \mu s$ for H RSE measurements) according to the SIMION simulations. Thus, by choosing the laser polarization along the TOF axis, our experiments are performed with the alignment close to the perpendicular direction, thus they can largely eliminate the contributions of dissociative ionization and CREI channels to the H RSE.

To further confirm this issue, we measure the angular distribution of the ionization and RSE at $\sim 200 \text{ TW/cm}^2$, i.e., the dependence of the yield on the angle between the direction of the laser polarization (\mathbf{E}) and the TOF axis. The results are presented in Fig. 5(a). To measure the angular distribution of direct ionization, a small slit is placed in front of the MCP detector to ensure that ions carrying kinetic energy can only be efficiently detected along the TOF axis, while for delayed ionization to detect RSE, no slit is used. One can see from the figure that unlike the near-isotropic angular distributions of the parent molecules H_2^+ and H_2^* (and the atoms Ar^+ and Ar^*), the angular distributions of fragments H^+ and H^* present strong anisotropic behavior. For H^+ fragments, the maximum distribution appears at $\mathbf{E} // \text{TOF}$, since they are mainly produced via BS and EI channels, and they prefer to eject along the laser polarization. On the other hand, the angular distribution of H^* exhibits the maximum at 90° and the minimum at 0° . Since energetic H^* fragments can only be efficiently detected at large angles in our PFI experimental setup, the results in Fig. 5(a) indicate that H^* produced via the BS or EI process is greatly suppressed by choosing laser polarization $\mathbf{E} // \text{TOF}$. We then measured the ellipticity dependence of RSE by fixing the major axis of the laser polarization parallel or perpendicular to the TOF axis. As shown in Fig. 5(b), while there are no apparent changes for H_2 RSE for both cases, the H RSE shows a much stronger ellipticity dependence when the major axis of the laser polarization is parallel to the TOF axis than that in the perpendicular case. This finding strongly indicates the different behaviors of H RSE with different alignments. In other words, the important role of recollision in the process of H RSE is revealed in the present study by the delayed ionization method and with the laser polarization parallel to the TOF axis, the experimental

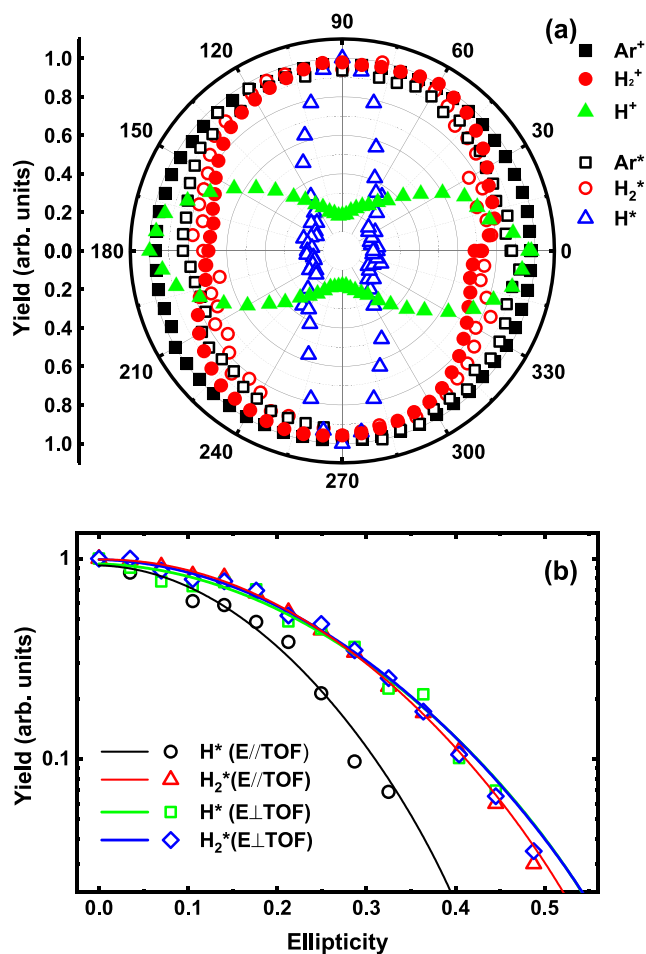


FIG. 5. (a) Dependence of the yields of Ar^+ (black solid square), H_2^+ (red solid circle), H^+ (green solid triangle), Ar^* (black hollow square), H_2^* (red hollow circle), and H^* (blue hollow triangle) on the angle between the laser polarization direction (\mathbf{E}) and the TOF axis. The angles 0° and 180° represent $\mathbf{E} // \text{TOF}$. (b) Ellipticity dependence of RSE by fixing the major axis of the laser polarization (\mathbf{E}) parallel or perpendicular to the TOF axis. Each solid line is the Gaussian fitting result of the experimental data. The laser intensity of (a) and (b) is kept at 200 TW/cm^2 .

setup of which is analogous to those that isolate the recollision process in strong field ionization [53,54,56,57].

We note that in addition to NSDI, another recollision-induced process could also be a possible mechanism to produce H^* , that is, the returning electron excites H_2^+ to the repulsive excited state, followed by dissociation to produce H^+ , which may be able to capture the electron forming the highly excited atom H^* . Recollision-induced excitation in H_2 molecules has been demonstrated in previous studies [53,54]. In the present study, while we cannot distinguish the atom RSE from the NSDI and recollision-induced excitation processes, we may tentatively exclude the latter based on the different ellipticity dependence of H^* for different laser intensities shown in Figs. 3(a) and 3(b). The SFA prediction shows a stronger ellipticity dependence at 500 TW/cm² than that at 200 TW/cm², which is opposite to the results of the H RSE. This can be easily understood as the H RSE is a frustrated dissociative DI process, which turns out to be a sequential one when the laser intensity is increased to 500 TW/cm², as we have discussed in the above sections.

The frustrated dissociative DI of molecules can be an analogy to the FDI process of atoms. For Ar atoms, a recent theoretical study has demonstrated that at moderate laser intensities, the FDI process is accompanied by NSDI, and the second electron prefers to be captured in a Rydberg state [25]. Our study indicates that recollision also plays an important role in the fragment RSE of a molecule. The results support the idea that the RESI pathway would be contributed to the H^* formation in a laser intensity around 200 TW/cm². Further studies would be of interest to reveal the mechanism of the coherent capture of electrons during breakup of the molecular bonds as well as the electron correlations in the fragment RSE formation of molecules.

IV. CONCLUSIONS

For summary, we present an experimental study on the RSE process of H_2 molecules in the tunneling ionization region. We observe that the neutral H_2 molecules can survive the strong 800-nm femtosecond laser fields in high Rydberg states. The H_2 Rydbergs generally behave similarly to its companion atom Ar, indicating the recapture mechanism of the molecular RSE. The RSE of the fragment H atoms is also identified. The dependence of H^* on both laser intensity and ellipticity strongly indicates that a frustrated dissociative NSDI process (i.e., upon NSDI the unstable doubly charged ion H_2^{2+} breaks up and one fragment H^+ captures a low-energy electron to form the highly excited H atom) is related to the fragment RSE of H_2 in strong laser fields. Our study shows that it is a general phenomenon of forming highly excited neutral parent molecules and fragments in strong laser fields, and it should stimulate further investigations to reveal the molecular orbital effect as well as the important role of recollision in the strong-field-induced RSE process of molecules.

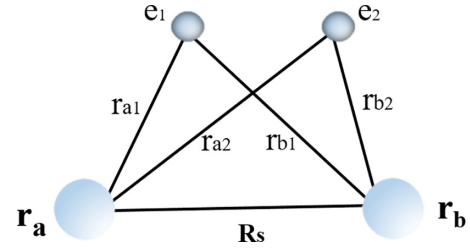


FIG. 6. The molecular structure of H_2 .

ACKNOWLEDGMENTS

This work was supported by the National Key program for S&T Research and Development (No. 2019YFA0307700), and the National Natural Science Foundation of China (Grants No. 12174148, No. 11874179, No. 12074144, and No. 12074146).

APPENDIX: THEORETICAL METHOD ON DOUBLE IONIZATION OF H_2

To explore the double ionization mechanism of H_2 molecules in intense laser fields, we utilized the classical ensemble method [58,59]. The structure of H_2 is shown as Fig. 6.

In the non-Born-Oppenheimer approximation, the classical Hamiltonian of 2D H_2 molecules in an intense laser field can be given by (atomic units are used throughout unless otherwise stated)

$$H_0 = \frac{P_a^2}{2m_p} + \frac{P_b^2}{2m_p} + \frac{p_1^2}{2m_e} + \frac{p_2^2}{2m_e} + \frac{1}{R} - \frac{1}{r_{a1}} - \frac{1}{r_{a2}} - \frac{1}{r_{b1}} - \frac{1}{r_{b2}}. \quad (A1)$$

Introducing the center-of-mass coordinates, since the mass of the nucleus is much larger than the electrons, we can approximately set the center of two nuclei as the coordinate origin, and the x -axis is along two nuclei. Thus, the Hamiltonian can be written as

$$H = \frac{P^2}{2\mu_P} + \frac{\sum_{ij} P_{ij}^2}{2\mu_e} + V_c(x, y, R_s) + V_{ex}(x, t) + V_{ey}(y, t), \quad (A2)$$

where the first and second terms are the kinetic energy of the nucleus and two electrons, $\mu_P = \frac{m_p}{2}$, $\mu_e = \frac{2m_p m_e}{2m_p + m_e}$ are the reduced mass; m_p and m_e are the masses of protons and electrons, respectively; R_s is the internuclear distance; $i = 1, 2$, $j = x, y$, x_1, x_2, y_1, y_2 are the electron coordinates; $P_{x_1}, P_{y_1}, P_{x_2}, P_{y_2}$ are the corresponding momentums; V_{ex}, V_{ey} are the laser fields; and the $V_c(x, y, R_s)$ is the potential energy, which

can be expressed as

$$V_c = V_{sc}(x, y, R_s) = \frac{1}{\sqrt{R_s^2 + \alpha_n^2}} - \frac{1}{\sqrt{(x_1 - 0.5R_s)^2 + y_1^2 + q_e^2}} - \frac{1}{\sqrt{(x_1 + 0.5R_s)^2 + y_1^2 + q_e^2}} - \frac{1}{\sqrt{(x_2 - 0.5R_s)^2 + y_2^2 + q_e^2}} - \frac{1}{\sqrt{(x_2 + 0.5R_s)^2 + y_2^2 + q_e^2}} + \frac{1}{\sqrt{(x_1 - x_2)^2 + (y_1 - y_2)^2 + b_e^2}}. \quad (\text{A3})$$

The soft parameters are $\alpha_n = 1$, $q_e = 1.25$, $b_e = 0.8$. By using the center-of-mass coordinates, Newton's equations can be transformed into Hamiltonian canonical equations

$$\frac{dr_{ij}}{dt} = \frac{\partial H}{\partial p_{ij}} = \frac{p_{ij}}{\mu_e}, \quad (\text{A4})$$

$$\frac{dp_{ij}}{dt} = -\frac{\partial H_{ij}}{\partial q_{ij}}, \quad (\text{A5})$$

$$\frac{dR_s}{dt} = \frac{P}{\mu_p}, \quad (\text{A6})$$

$$\frac{\partial P}{\partial t} = -\frac{\partial V_{sc}}{V_{R_s}}. \quad (\text{A7})$$

The symplectic method is the difference method, which is suitable for the long-time many-step calculations. We chose a set of initial stable states by the Monte Carlo method and solved the above canonical equations numerically in order to obtain the time evolutions of the electron positions and the corresponding momenta. Since the Hamiltonian system (2) is a separable Hamiltonian system, we may use the four-stage

fourth-order explicit symplectic scheme to solve it [59]. In our calculation, we assumed that the initial ensemble has the same energy equal to the ground-state energies of the H₂ molecule (1.16 a.u.) with the equilibrium nucleus distance $R = 1.4$ a.u. We utilized a microcanonical ensemble that consisted of 2×10^6 two-electron trajectories.

The external laser pulse can be expressed as follows:

$$E_x = E_0 f(t) \frac{1}{\sqrt{1 + \varepsilon^2}} \cos(\omega t + \varphi) \hat{e}_x, \quad (\text{A8})$$

$$E_y = E_0 f(t) \frac{\varepsilon}{\sqrt{1 + \varepsilon^2}} \sin(\omega t + \varphi) \hat{e}_y, \quad (\text{A9})$$

$f(t)$ is the laser envelope, the pulse duration $T = 10T_0$, with $T_0 = 2\pi/\omega_0$ being the period of the pulse, and E_0 is the peak intensity, with the frequency $\omega_0 = 0.057$ a.u. (800 nm in wavelength), which is in accordance with the experimental condition. $\varepsilon = 0$ and 1 presents the linearly and circularly polarized laser fields, respectively.

-
- [1] P. B. Corkum, *Phys. Rev. Lett.* **71**, 1994 (1993).
[2] K. J. Schafer, B. Yang, L. F. DiMauro, and K. C. Kulander, *Phys. Rev. Lett.* **70**, 1599 (1993).
[3] M. Ferray, A. L'Huillier, X. F. Li, L. A. Lompre, G. Mainfray, and C. Manus, *J. Phys. B* **21**, L31 (1988).
[4] Y. Qiao, Y.-Q. Huo, S.-C. Jiang, Y.-J. Yang, and J.-G. Chen, *Opt. Express* **30**, 9971 (2022).
[5] G. G. Paulus, W. Nicklich, H. Xu, P. Lambropoulos, and H. Walther, *Phys. Rev. Lett.* **72**, 2851 (1994).
[6] D. B. Milošević, G. G. Paulus, D. Bauer, and W. Becker, *J. Phys. B* **39**, R203 (2006).
[7] W. Becker, X. J. Liu, P. J. Ho, and J. H. Eberly, *Rev. Mod. Phys.* **84**, 1011 (2012).
[8] B.-B. Wang, X.-F. Li, P.-M. Fu, C. Jing, and L. Jie, *Chin. Phys. Lett.* **23**, 2729 (2006).
[9] T. Nubbemeyer, K. Gorling, A. Saenz, U. Eichmann, and W. Sandner, *Phys. Rev. Lett.* **101**, 233001 (2008).
[10] U. Eichmann, T. Nubbemeyer, H. Rottke, and W. Sandner, *Nature (London)* **461**, 1261 (2009).
[11] C. Maher-McWilliams, P. Douglas, and P. F. Barker, *Nat. Photon.* **6**, 386 (2012).
[12] H. Yun, J. H. Mun, S. I. Hwang, S. B. Park, I. A. Ivanov, and C. H. Nam, *Nat. Photon.* **12**, 620 (2018).
[13] M. Matthews, F. Morales, A. Patas, A. Lindinger, J. Gateau, and N. Berti, *Nat. Phys.* **14**, 695 (2018).
[14] J. H. Mun, I. A. Ivanov, H. Yun, and K. T. Kim, *Phys. Rev. A* **98**, 063429 (2018).
[15] L. Ortmann, C. Hofmann, I. A. Ivanov, and A. S. Landsman, *Phys. Rev. A* **103**, 063112 (2021).
[16] H. Zimmermann, J. Buller, S. Eilzer, and U. Eichmann, *Phys. Rev. Lett.* **114**, 123003 (2015).
[17] S. P. Xu, M. Q. Liu, S. L. Hu, Z. Shu, W. Quan, Z. L. Xiao, Y. Zhou, M. Z. Wei, M. Zhao, R. P. Sun, Y. L. Wang, L. Q. Hua, C. Gong, X. Y. Lai, J. Chen, and X. J. Liu, *Phys. Rev. A* **102**, 043104 (2020).
[18] F. Sun, C. Lu, Y. Ma, S. Pan, J. Wang, W. Zhang, J. Qiang, F. Chen, H. Ni, H. Li, and J. Wu, *Opt. Express* **29**, 31240 (2021).
[19] A. S. Landsman, A. N. Pfeiffer, C. Hofmann, M. Smolarski, C. Cirelli, and U. Keller, *New J. Phys.* **15**, 013001 (2013).
[20] Q. Z. Xia, L. B. Fu, and J. Liu, *Phys. Rev. A* **87**, 033404 (2013).
[21] H. Zimmermann, S. Patchkovskii, M. Ivanov, and U. Eichmann, *Phys. Rev. Lett.* **118**, 013003 (2017).
[22] S. Hu, X. Hao, H. Lv, M. Liu, T. Yang, H. Xu, M. Jin, D. Ding, Q. Li, W. Li, W. Becker, and J. Chen, *Opt. Express* **27**, 31629 (2019).
[23] S. Larimian, S. Erattupuzha, C. Lemell, S. Yoshida, S. Nagele, R. Maurer, A. Baltuška, J. Burgdörfer, M. Kitzler, and X. Xie, *Phys. Rev. A* **94**, 033401 (2016).
[24] S. Larimian, S. Erattupuzha, A. Baltuška, M. Kitzler-Zeiler, and X. Xie, *Phys. Rev. Res.* **2**, 013021 (2020).

- [25] S. Chen, J. Chen, G. G. Paulus, and H. P. Kang, *Phys. Rev. A* **102**, 023103 (2020).
- [26] A. Emmanouilidou, C. Lazarou, A. Staudte, and U. Eichmann, *Phys. Rev. A* **85**, 011402(R) (2012).
- [27] B. Manschwetus, T. Nubbemeyer, K. Gorling, G. Steinmeyer, U. Eichmann, H. Rottke, and W. Sandner, *Phys. Rev. Lett.* **102**, 113002 (2009).
- [28] J. McKenna, S. Zeng, J. J. Hua, A. M. Sayler, M. Zohrabi, N. G. Johnson, B. Gaire, K. D. Carnes, B. D. Esry, and I. Ben-Itzhak, *Phys. Rev. A* **84**, 043425 (2011).
- [29] W. Zhang, H. Li, X. Gong, P. Lu, Q. Song, Q. Ji, K. Lin, J. Ma, H. Li, F. Sun, J. Qiang, H. Zeng, and J. Wu, *Phys. Rev. A* **98**, 013419 (2018).
- [30] T. Nubbemeyer, U. Eichmann, and W. Sandner, *J. Phys. B* **42**, 134010 (2009).
- [31] W. Zhang, P. Lu, X. Gong, H. Li, Q. Ji, K. Lin, J. Ma, H. Li, F. Sun, J. Qiang, F. Chen, J. Tong, and J. Wu, *Phys. Rev. A* **101**, 033401 (2020).
- [32] J. Ma, W. Zhang, K. Lin, Q. Ji, H. Li, F. Sun, J. Qiang, F. Chen, J. Tong, P. Lu, H. Li, X. Gong, and J. Wu, *Phys. Rev. A* **100**, 063413 (2019).
- [33] J. Wu, A. Vredenburg, B. Ulrich, L. P. H. Schmidt, M. Meckel, S. Voss, H. Sann, H. Kim, T. Jahnke, and R. Dörner, *Phys. Rev. Lett.* **107**, 043003 (2011).
- [34] F. Sun, W. Zhang, P. Lu, Q. Song, K. Lin, Q. Ji, J. Ma, H. Li, J. Qiang, X. Gong, H. Li, and J. Wu, *J. Phys. B* **53**, 035601 (2020).
- [35] X. Xie, C. Wu, H. Liu, M. Li, Y. Deng, Y. Liu, Q. Gong, and C. Wu, *Phys. Rev. A* **88**, 065401 (2013).
- [36] D. B. Milošević, *Phys. Rev. A* **74**, 063404 (2006).
- [37] D. Pavičić, K. F. Lee, D. M. Rayner, P. B. Corkum, and D. M. Villeneuve, *Phys. Rev. Lett.* **98**, 243001 (2007).
- [38] Z. Y. Lin, X. Y. Jia, C. L. Wang, Z. L. Hu, H. P. Kang, W. Quan, X. Y. Lai, X. J. Liu, J. Chen, B. Zeng, W. Chu, J. P. Yao, Y. Cheng, and Z. Z. Xu, *Phys. Rev. Lett.* **108**, 223001 (2012).
- [39] J. Yao, G. Li, X. Jia, X. Hao, B. Zeng, C. Jing, W. Chu, J. Ni, H. Zhang, H. Xie, C. Zhang, Z. Zhao, J. Chen, X. Liu, Y. Cheng, and Z. Xu, *Phys. Rev. Lett.* **111**, 133001 (2013).
- [40] M. Lein, N. Hay, R. Velotta, J. P. Marangos, and P. L. Knight, *Phys. Rev. Lett.* **88**, 183903 (2002).
- [41] H. Lv, W. Zuo, L. Zhao, H. Xu, M. Jin, D. Ding, S. Hu, and J. Chen, *Phys. Rev. A* **93**, 033415 (2016).
- [42] M. V. Ammosov, N. B. Delone, and V. P. Krainov, *Zh. Eksp. Teor. Fiz.* **91**, 2008 (1986) [*Sov. Phys. JETP* **64**, 1191 (1986)].
- [43] A. Talebpour, S. Laroche, and S. L. Chin, *J. Phys. B* **31**, L49 (1998).
- [44] E. Wells, M. J. DeWitt, and R. R. Jones, *Phys. Rev. A* **66**, 013409 (2002).
- [45] X. M. Tong, Z. X. Zhao, and C. D. Lin, *Phys. Rev. A* **66**, 033402 (2002).
- [46] A. Saenz, *J. Phys. B* **33**, 4365 (2000).
- [47] T. K. Kjeldsen and L. B. Madsen, *Phys. Rev. A* **71**, 023411 (2005).
- [48] V. I. Usachenko and S.-I. Chu, *Phys. Rev. A* **71**, 063410 (2005).
- [49] J. R. Bettis, *Phys. Rev. A* **80**, 063420 (2009).
- [50] L. Zhao, J. Dong, H. Lv, T. Yang, Y. Lian, M. Jin, H. Xu, D. Ding, S. Hu, and J. Chen, *Phys. Rev. A* **94**, 053403 (2016).
- [51] A. Staudte, C. Ruiz, M. Schöffler, S. Schössler, D. Zeidler, T. Weber, M. Meckel, D. M. Villeneuve, P. B. Corkum, A. Becker, and R. Dörner, *Phys. Rev. Lett.* **99**, 263002 (2007).
- [52] A. Rudenko, V. L. B. de Jesus, T. Ergler, K. Zrost, B. Feuerstein, C. D. Schröter, R. Moshhammer, and J. Ullrich, *Phys. Rev. Lett.* **99**, 263003 (2007).
- [53] H. Niikura, F. Légaré, R. Hasbani, A. D. Bandrauk, M. Y. Ivanov, D. M. Villeneuve, and P. B. Corkum, *Nature (London)* **417**, 917 (2002).
- [54] H. Niikura, F. Légaré, R. Hasbani, M. Y. Ivanov, D. M. Villeneuve, and P. B. Corkum, *Nature (London)* **421**, 826 (2003).
- [55] J. Muth-Böhm, A. Becker, and F. H. M. Faisal, *Phys. Rev. Lett.* **85**, 2280 (2000).
- [56] A. S. Alnaser, T. Osipov, E. P. Benis, A. Wech, B. Shan, C. L. Cocke, X. M. Tong, and C. D. Lin, *Phys. Rev. Lett.* **91**, 163002 (2003).
- [57] A. S. Alnaser, X. M. Tong, T. Osipov, S. Voss, C. M. Maharjan, P. Ranitovic, B. Ulrich, B. Shan, Z. Chang, C. D. Lin, and C. L. Cocke, *Phys. Rev. Lett.* **93**, 183202 (2004).
- [58] W. Zuo, S. Ben, H. Lv, L. Zhao, J. Guo, X.-S. Liu, H. Xu, M. Jin, and D. Ding, *Phys. Rev. A* **93**, 053402 (2016).
- [59] X. S. Liu, Y. Y. Qi, J. F. He, and P. Z. Ding, *Commun. Comput. Phys.* **2**, 1 (2007).